JACS
JOURNAL OF THE AMERICAN CHEMICAL SOCIETY
Communication
Cite This: J. Am. Chem. Soc. 2019, 141, 19542−19545
pubs.acs.org/JACS

In Situ Production of Ag/Polymer Asymmetric Nanoparticles via a Powerful Light-Driven Technique

Richen Li,[†] Hai Wang,[†] Yue Song,[†] Yen-Nan Lin,[†,#] Mei Dong,[†] Yidan Shen,[†] Sarosh Khan,[†] Shiyi Zhang,[†] Jingwei Fan,[†] Fuwu Zhang,[†] Lu Su,*[,†] and Karen L. Wooley*[,†]

[†]Departments of Chemistry, Chemical Engineering and Materials Science & Engineering, Texas A&M University, College Station, Texas 77842, United States

[#]College of Medicine, Texas A&M University, Bryan, Texas 77807, United States

Supporting Information

ABSTRACT: As a rapid, controllable, and easily transferrable approach to the preparation of antimicrobial nanoparticle systems, a one-step, light-driven procedure was developed to produce asymmetric hybrid inorganic−organic nanoparticles (NPs) directly from a homogeneous Ag/polymer mixture. An amphiphilic triblock polymer was designed and synthesized to build biocompatible NPs, consisting of poly(ethylene oxide) (PEO), carboxylic acid-functionalized polyphosphoester (PPE), and poly(L-lactide) (PLLA). Unexpectedly, snowman-like asymmetric nanostructures were subsequently obtained by simply loading silver cations into the polymeric micelles together with purification via centrifugation. With an understanding of the chemistry of the asymmetric NP formation, a controllable preparation strategy was developed by applying UV irradiation. A morphology transition was observed by transmission electron microscopy over the UV irradiation time, from small silver NPs distributed inside the micelles into snowman-like asymmetric NPs, which hold promise for potential antimicrobial applications with their unique two-stage silver release profiles.

Asymmetric nanoparticles (NPs) have been investigated extensively owing to their unique anisotropic features in composition, morphology, and properties.[1−6] Throughout the past three decades, a variety of strategies have been developed for the synthesis of asymmetric NPs, e.g., surface modification and compartmentalization.[7−16] The one-step fabrication of well-defined asymmetric NPs in a straightforward and efficient manner, however, remains a challenge.[17,18] Herein, through rational design of the chemical structures of each segment, a well-defined biocompatible amphiphilic polymer was prepared, which was unexpectedly capable of generating snowman-like asymmetric nanostructures from a homogeneous Ag/polymer mixture. Moreover, based on our hypothesized mechanism for the NP formation, an accelerated light-driven approach to produce the asymmetric NPs was further developed.

Our initial intention was to construct biocompatible NPs and load them with silver cations to serve as antimicrobial nanomedical devices. Therefore, an amphiphilic triblock polymer (Scheme 1) was designed and synthesized, consisting of poly(ethylene oxide) (PEO), carboxylic acid-functionalized polyphosphoester (PPE), and poly(L-lactide) (PLLA) segments.[19,20] In contrast to our earlier studies involving PPEs,[21,22] a novel cyclic phosphotriester monomer, 2-ethoxy-4-vinyl-1,3,2-dioxaphospholane-2-oxide (E4VP, Figure S1), was designed. This monomer carried a reactive vinylic group on the phospholane ring to allow for chemical modification of resulting polymers, while avoiding the production of ethylene glycol as a known toxic hydrolytic degradation product.

The amphiphilic polymer, $mPEO_{45}$-*b*-PE4VP$(COOH)_{50}$-*b*-$PLLA_{20}$, was then prepared by a rapid organobase-catalyzed one-pot sequential ring-opening polymerization (ROP) of E4VP and L-lactide, with methoxy PEO ($mPEO_{45}$) as the macroinitiator, followed by postpolymerization modification with 3-mercaptopropionic acid via a photoinitiated thiol−ene click reaction (Scheme 1, Figures S2 and S3). Importantly, the PPE segment of the triblock terpolymer contained only a single thioether and carboxylic acid at each repeat unit, giving weaker interactions with metal ions, such as silver cations, relative to our previously reported PPEs. The weaker interactions were expected to render Ag/polymer mixtures more prone to reduction.[23] The amphiphilic polymer was capable of self-assembling into spherical core−shell−corona micelles by direct dissolution in MOPS buffer (pH = 7.4). As depicted in Figure S4a, the transmission electron microscopy (TEM) image displayed circular structures of the NPs with an average diameter (D_{av}) of 17 ± 3 nm. Dynamic light scattering (DLS) showed a unimodal size distribution, with a number-averaged hydrodynamic diameter ($D_{h(number)}$) of 21 ± 8 nm (Figure S4b). The biocompatibility of the micelles was confirmed by cytotoxicity studies against the RAW 264.7 mouse macrophage cell line, which showed negligible cytotoxicity up to a concentration of 750 μg/mL (Figure S4c).

Unexpected snowman-like asymmetric NPs were subsequently obtained, through simply loading silver cations into the $mPEO_{45}$-*b*-PE4VP$(COOH)_{50}$-*b*-$PLLA_{20}$ micelles followed by purification of the NPs via centrifugation. The asymmetric NPs consisted of two circular parts observed in the two-dimensional TEM image (Figure 1a) with similar D_{av} of ca. 14 nm. Those two domains exhibited different degrees of contrast under TEM. The higher contrast portion of the asymmetric NPs in the TEM image comprised metallic silver reduced from silver

Received: September 20, 2019
Published: December 10, 2019

DOI: 10.1021/jacs.9b10205
J. Am. Chem. Soc. 2019, 141, 19542−19545

Scheme 1. Synthesis of Polymer 1, mPEO$_{45}$-*b*-PE4VP$_{50}$-*b*-PLLA$_{20}$, Followed by Postpolymerization Modification *via* a Thiol–Ene Click Reaction with 3-Mercaptopropionic Acid to Prepare Polymer 2, mPEO$_{45}$-*b*-PE4VP(COOH)$_{50}$-*b*-PLLA$_{20}$

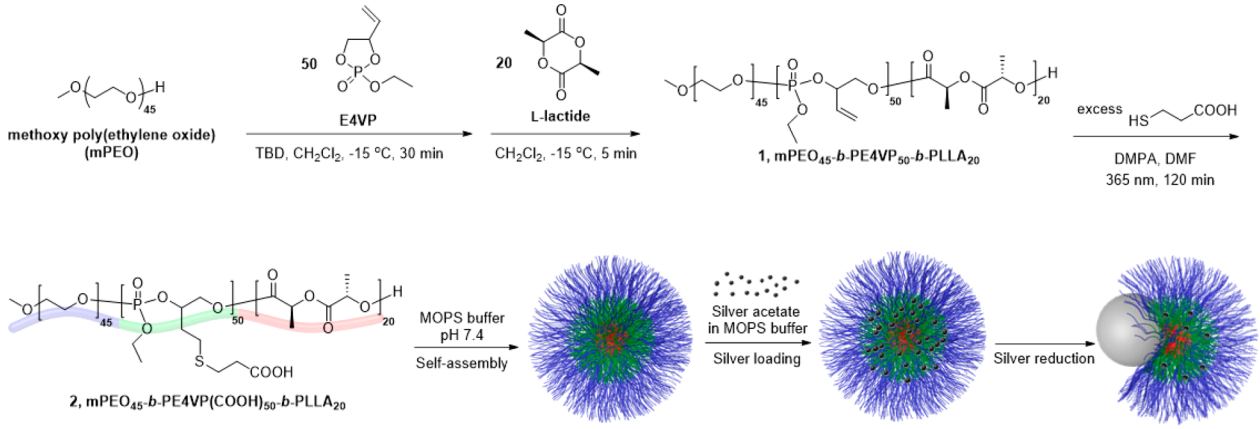

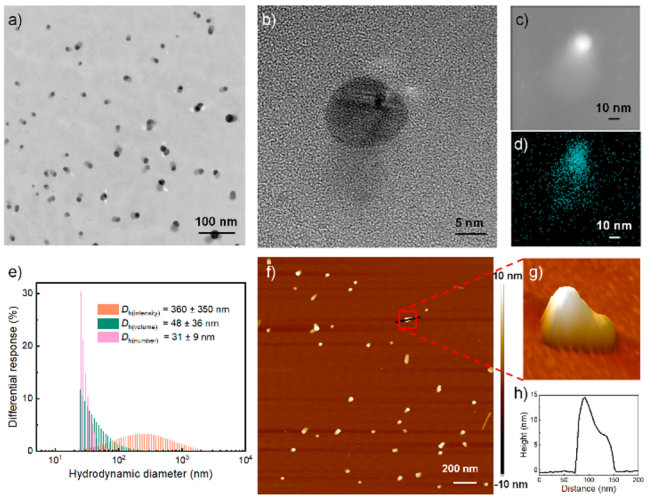

Figure 1. Characterization of the composite Ag/polymer asymmetric NPs prepared by loading silver cations into the polymeric micelles followed by purification via centrifugation. EM images after drop deposition onto carbon-coated copper grids with no staining: (a) TEM; (b) HRTEM; (c) STEM; and (d) elemental (Ag) mapping by EDX. (e) Number-, volume-, and intensity-averaged hydrodynamic diameter histograms measured by DLS. AFM imaging after drop deposition onto freshly cleaved mica and drying under ambient conditions: (f) AFM image of many asymmetric NPs with one NP selected for 3D view (g) and height profile analysis (h).

cations, as confirmed by high-resolution TEM (HRTEM, Figure 1b) and energy-dispersive X-ray spectroscopy (EDX) elemental mapping analysis (Figures 1d and S5). The region of each asymmetric NP having lower contrast contained relatively low amounts of silver and was expected to be composed primarily of polymer material. Compared to the empty micelles, DLS results indicated an increase of the $D_{h(number)}$ to 31 ± 9 nm for the composite Ag/polymer asymmetric NPs (Figures 1e and S4b). The asymmetric nanostructure was further confirmed by atomic force microscopy (AFM), which revealed average heights of the two components to be 14 ± 4 nm and 6 ± 2 nm, respectively (Figure 1f–h). It is hypothesized that parts of the silver cations were reduced to form small silver NPs due to the relatively weak interactions, which was triggered and accelerated by the centrifugation process. The intrinsic flexibility of the polymer chain, indicated by the low T_g (− 20 °C) of the polymer, allowed for the growth and fusion of the small silver NPs, accompanied by phase separation, to form the asymmetric NPs. Meanwhile, the peripheral hydrophilic PEO segment prevented further aggregation/precipitation of the NPs.

With an understanding of the chemistry of the asymmetric NPs, a more controllable preparation strategy was further developed, taking advantage of the light sensitivity of silver cations.[24] Solutions of mPEO$_{45}$-*b*-PE4VP(COOH)$_{50}$-*b*-PLLA$_{20}$ and silver acetate in MOPS buffer were mixed and allowed to stir under UV irradiation (365 nm, 500 μJ/cm^2) for 2, 4, 6, and 10 min, respectively. As characterized by TEM (Figures 2 and S6) without staining, in the absence of UV irradiation and without centrifugation, Ag/polymer NPs originating from reduction of silver cations were rarely observed. After 2 min of UV irradiation, small silver NPs appeared within the frameworks of the micelles. A morphology transition from small silver NPs distributed inside the micelles (2 min) into snowman-like asymmetric NPs (6 min) was observed with increasing irradiation time. However, large aggregates were observed at >10 min UV irradiation, probably due to the secondary hierarchical assembly of the asymmetric NPs arising from the incomplete hydrophilic PEO shielding for the reduced silver species (Figure S6). In comparison, under the same conditions without the polymer as a stabilizing agent, solutions of silver acetate in MOPS buffer did not generate well-defined asymmetric NPs (Figure S7). Rather, macroscopic precipitates formed in the solution within 1 d. The reduction of Ag^+ into Ag^0 over time under UV irradiation was confirmed by X-ray photoelectron spectroscopy (Figure S8).

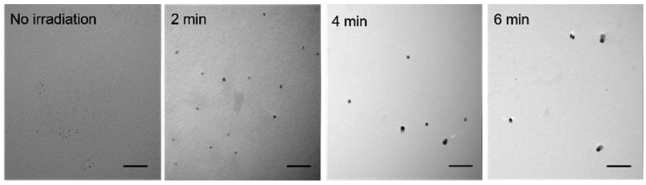

Figure 2. TEM images of the mixture of polymer 2 and silver acetate solutions in the MOPS buffer (pH = 7.4) and the mixtures irradiated by UV for 2, 4, and 6 min, respectively. Scale bar: 100 nm.

The resulting asymmetric NPs were further evaluated by determining their silver release profiles against nanopure water to investigate the structure–property relationships (Figure S9). Dialysis cassettes were used to monitor the decrease of silver

DOI: 10.1021/jacs.9b10205
J. Am. Chem. Soc. 2019, 141, 19542–19545

concentration upon dialysis against nanopure water (pH ca. 5.5−6). Under these conditions, it was expected that Ag^+ could be released relatively quickly, whereas Ag^0 would undergo oxidation and be released over time.[25] At 37 °C, the asymmetric NPs showed an initial burst release (ca. 50%) of silver within 2 h, followed by a more controlled and sustained release of the remaining silver over ca. 2 d. In comparison, complete release of silver from a silver acetate control solution was observed within 1 h. The two-stage silver release profile supported the observed asymmetric nanostructure, which is also anticipated to be beneficial for the treatment of bacterial infections.[26]

In conclusion, a serendipitous observation led to the development of a facile and rapid supramolecular assembly combined with a light-driven approach to fabricate Ag/polymer asymmetric NPs. Acceleration and control were achieved by UV irradiation of Ag/polymer mixtures, with the reaction progress depending on the extent of UV exposure. The convenient synthesis and unique two-stage silver release profile demonstrate the promise of these asymmetric NPs as potential antimicrobial agents.

■ ASSOCIATED CONTENT

Supporting Information

The Supporting Information is available free of charge at https://pubs.acs.org/doi/10.1021/jacs.9b10205.

Experimental procedures, figures, and additional data (PDF)

■ AUTHOR INFORMATION

Corresponding Authors

*l.su@tue.nl

*wooley@chem.tamu.edu

ORCID

Hai Wang: 0000-0002-1215-2613

Yue Song: 0000-0002-7800-5528

Mei Dong: 0000-0002-9862-0296

Lu Su: 0000-0001-8207-756X

Karen L. Wooley: 0000-0003-4086-384X

Notes

The authors declare no competing financial interest.

■ ACKNOWLEDGMENTS

We gratefully acknowledge financial support from National Heart Lung and Blood Institute of the National Institutes of Health as a Program of Excellence in Nanotechnology (HHSN268201000046C), the National Science Foundation (CHE-1610311, DMR-1905818, and DMREF-1629094), and the Robert A. Welch Foundation through the W. T. Doherty-Welch Chair in Chemistry (A-0001). The Laboratory for Synthetic-Biologic Interactions (LSBI) at Texas A&M University is also acknowledged. We thank Dr. Hansoo Kim and the Microscopy Imaging Center at Texas A&M University for assistance with HRTEM and EDX measurements. Use of the TAMU Materials Characterization Facility is acknowledged.

■ REFERENCES

(1) Chen, P.-C.; Liu, M.; Du, J. S.; Meckes, B.; Wang, S.; Lin, H.; Dravid, V. P.; Wolverton, C.; Mirkin, C. A. Interface and Heterostructure Design in Polyelemental Nanoparticles. *Science* **2019**, *363*, 959−964.

(2) Du, J.; O'Reilly, R. K. Anisotropic Particles with Patchy, Multicompartment and Janus Architectures: Preparation and application. *Chem. Soc. Rev.* **2011**, *40*, 2402−2416.

(3) Walther, A.; Müller, A. H. E. Janus Particles: Synthesis, self-Assembly, physical properties, and applications. *Chem. Rev.* **2013**, *113*, 5194−5261.

(4) Zhao, T.; Chen, L.; Wang, P.; Li, B.; Lin, R.; Al-Khalaf, A. A.; Hozzein, W. N.; Zhang, F.; Li, X.; Zhao, D. Surface-kinetics Mediated Mesoporous Multipods for Enhanced Bacterial Adhesion and Inhibition. *Nat. Commun.* **2019**, *10*, 4387.

(5) Singh, K.; Raghav, A.; Jha, P. K.; Satapathi, S. Effect of Size and Charge Asymmetry on Aggregation Kinetics of Oppositely Charged Nanoparticles. *Sci. Rep.* **2019**, *9*, 3762.

(6) Guo, Z. H.; Le, A. N.; Feng, X.; Choo, Y.; Liu, B.; Wang, D.; Wan, Z.; Gu, Y.; Zhao, J.; Li, V. Janus Graft Block Copolymers: Design of a polymer architecture for independently tuned nanostructures and polymer properties. *Angew. Chem., Int. Ed.* **2018**, *57*, 8493−8497.

(7) Fan, X.; Yang, J.; Loh, X. J.; Li, Z. Polymeric Janus Nanoparticles: Recent advances in synthetic strategies, materials properties, and applications. *Macromol. Rapid Commun.* **2019**, *40*, 1800203.

(8) Gröschel, A. H.; Walther, A.; Löbling, T. I.; Schmelz, J.; Hanisch, A.; Schmalz, H.; Müller, A. H. Facile, Solution-based Synthesis of Soft, Nanoscale Janus Particles with Tunable Janus balance. *J. Am. Chem. Soc.* **2012**, *134*, 13850−13860.

(9) Lattuada, M.; Hatton, T. A. Preparation and Controlled Self-assembly of Janus Magnetic Nanoparticles. *J. Am. Chem. Soc.* **2007**, *129*, 12878−12889.

(10) Zhang, S.; Li, Z.; Samarajeewa, S.; Sun, G.; Yang, C.; Wooley, K. L. Orthogonally Dual-clickable Janus Nanoparticles *via* a Cyclic Templating Strategy. *J. Am. Chem. Soc.* **2011**, *133*, 11046−11049.

(11) Zhang, Z.; Li, H.; Huang, X.; Chen, D. Solution-Based Thermodynamically Controlled Conversion from Diblock Copolymers to Janus Nanoparticles. *ACS Macro Lett.* **2017**, *6*, 580−585.

(12) Kim, Y.; Macfarlane, R. J.; Jones, M. R.; Mirkin, C. A. Transmutable Nanoparticles with Reconfigurable Surface Ligands. *Science* **2016**, *351*, 579−582.

(13) Hayes, O. G.; McMillan, J. R.; Lee, B.; Mirkin, C. A. DNA-encoded Protein Janus Nanoparticles. *J. Am. Chem. Soc.* **2018**, *140*, 9269−9274.

(14) Lin, Y.; Thomas, M. R.; Gelmi, A.; Leonardo, V.; Pashuck, E. T.; Maynard, S. A.; Wang, Y.; Stevens, M. M. Self-assembled 2D Free-standing Janus Nanosheets with Single-layer Thickness. *J. Am. Chem. Soc.* **2017**, *139*, 13592−13595.

(15) Wang, Z.; Wang, Z.; Li, J.; Cheung, S. T. H.; Tian, C.; Kim, S.-H.; Yi, G.-R.; Ducrot, E.; Wang, Y. Active Patchy Colloids with Shape-Tunable Dynamics. *J. Am. Chem. Soc.* **2019**, *141*, 14853−14863.

(16) Sadtler, B.; Demchenko, D. O.; Zheng, H.; Hughes, S. M.; Merkle, M. G.; Dahmen, U.; Wang, L.-W.; Alivisatos, A. P. Selective Facet Reactivity During Cation Exchange in Cadmium Sulfide Nanorods. *J. Am. Chem. Soc.* **2009**, *131*, 5285−5293.

(17) Wang, Y.; Ding, T.; Baumberg, J. J.; Smoukov, S. K. Symmetry Breaking Polymerization: One-pot synthesis of plasmonic hybrid Janus nanoparticles. *Nanoscale* **2015**, *7*, 10344−10349.

(18) Xie, H.; She, Z.-G.; Wang, S.; Sharma, G.; Smith, J. W. One-step Fabrication of Polymeric Janus Nanoparticles for Drug Delivery. *Langmuir* **2012**, *28*, 4459−4463.

(19) Schöttler, S.; Becker, G.; Winzen, S.; Steinbach, T.; Mohr, K.; Landfester, K.; Mailänder, V.; Wurm, F. R. Protein Adsorption Is Required for Stealth Effect of Poly(ethylene glycol)- and Poly(phosphoester)-coated nanocarriers. *Nat. Nanotechnol.* **2016**, *11*, 372−377.

(20) Ramot, Y.; Haim-Zada, M.; Domb, A. J.; Nyska, A. Biocompatibility and Safety of PLA and Its Copolymers. *Adv. Drug Delivery Rev.* **2016**, *107*, 153−162.

DOI: 10.1021/jacs.9b10205
J. Am. Chem. Soc. 2019, 141, 19542−19545

(21) Lim, Y. H.; Tiemann, K. M.; Heo, G. S.; Wagers, P. O.; Rezenom, Y. H.; Zhang, S.; Zhang, F.; Youngs, W. J.; Hunstad, D. A.; Wooley, K. L. Preparation and *in vitro* Antimicrobial Activity of Silver-Bearing Degradable Polymeric Nanoparticles of Polyphosphoester-*block*-Poly(L-lactide). *ACS Nano* **2015**, *9*, 1995−2008.
(22) Chen, Q.; Shah, K. N.; Zhang, F.; Salazar, A. J.; Shah, P. N.; Li, R.; Sacchettini, J. C.; Wooley, K. L.; Cannon, C. L. Minocycline and Silver Dual-loaded Polyphosphoester-based Nanoparticles for Treatment of Resistant *Pseudomonas Aeruginosa*. *Mol. Pharmaceutics* **2019**, *16*, 1606−1619.
(23) Liau, S.; Read, D.; Pugh, W.; Furr, J.; Russell, A. Interaction of Silver Nitrate with Readily Identifiable Groups: Relationship to the antibacterialaction of silver ions. *Lett. Appl. Microbiol.* **1997**, *25*, 279−283.
(24) Tan, C.; Qin, C.; Sadtler, B. Light-directed Growth of Metal and Semiconductor Nanostructures. *J. Mater. Chem. C* **2017**, *5*, 5628−5642.
(25) Kittler, S.; Greulich, C.; Diendorf, J.; Koller, M.; Epple, M. Toxicity of Silver Nanoparticles Increases During Storage because of Slow Dissolution under Release of Silver Ions. *Chem. Mater.* **2010**, *22*, 4548−4554.
(26) Sambhy, V.; MacBride, M. M.; Peterson, B. R.; Sen, A. Silver Bromide Nanoparticle/Polymer Composites: Dual action tunable antimicrobial materials. *J. Am. Chem. Soc.* **2006**, *128*, 9798−9808.

DOI: 10.1021/jacs.9b10205
J. Am. Chem. Soc. 2019, 141, 19542−19545